nature immunology

Secondary T cell–T cell synaptic interactions drive the differentiation of protective CD8+ T cells

Audrey Gérard[1], Omar Khan[1], Peter Beemiller[1], Erin Oswald[1], Joyce Hu[2], Mehrdad Matloubian[2] & Matthew F Krummel[1]

Immunization results in the differentiation of CD8+ T cells, such that they acquire effector abilities and convert into a memory pool. Priming of T cells takes place via an immunological synapse formed with an antigen-presenting cell (APC). By disrupting synaptic stability at different times, we found that the differentiation of CD8+ T cells required cell interactions beyond those made with APCs. We identified a critical differentiation period that required interactions between primed T cells. We found that T cell–T cell synapses had a major role in the generation of protective CD8+ T cell memory. T cell–T cell synapses allowed T cells to polarize critical secretion of interferon-γ (IFN-γ) toward each other. Collective activation and homotypic clustering drove cytokine sharing and acted as regulatory stimuli for T cell differentiation.

Effective adaptive immunity relies on the ability of lymphocytes to differentiate and to make a concerted response. An immune response requires a few specific T cells not only to find rare cognate antigen-presenting cells (APCs) but also to receive appropriate signals to differentiate into effector or memory subsets. Much work has focused on determining how the appropriate amount of antigen, its affinity for the T cell antigen receptor (TCR) or the requirement of costimulation during a priming APC encounter regulates optimal T cell differentiation. However, proper differentiation of CD8+ T cells requires other signals, such as help from CD4+ T cells and cytokines[1–3]. Despite considerable work, the timing, site and conditions of CD8+ T cell differentiation remain unknown[3–5].

Priming of CD8+ T cells occurs in many ways, and the requirement for particular cytokines or costimulators may be overcome by alternative pathways[4]. As a result, the populations of antigen-specific CD8+ T cells formed are heterogeneous[6], and not all T cells, even those bearing the same TCR, will evolve similarly. Despite some heterogeneity, CD8+ T cells mostly respond in an integrated manner, but how they coordinate their response is elusive. Furthermore, only a few T cells are needed to mount an efficient and coordinated immune response, and a high frequency of precursor cells is not beneficial. Various lines of evidence suggest that T cells have developed strategies for finding other activated T cells[7,8], exchanging information[9] and acting cooperatively[10].

Advances in two-photon imaging have permitted direct observation of T cell activity during an immune response in lymph nodes. After recognition of their cognate antigen presented by a dendritic cell (DC), T cells slow down and form long stable interactions with DCs[11–14]. During this arrest phase, also called 'phase II'[11], several T cells are often found interacting with the same APC, forming clusters[15]. During clustering events, it has been noted that T cells may interact with each other[16,17]. *In vitro*, CD4+ T cells form synapses in which more localized interleukin 2 (IL-2) signaling complexes are found[9,18]. The implication of such interactions for T cell responses *in vivo*, however, has not yet been assessed.

Here we provide evidence of a critical differentiation period (CDP) for CD8+ T cells during the course of an immune response. We found that cell-cell interactions beyond T cell–APC interactions were necessary, at physiological precursor frequencies, to generate optimal CD8+ T cell responses. We also found that mutual adherence and synapses between T cells was one of the cell-cell interactions required for CD8+ T cell differentiation. T cell–T cell synaptic structures thus provide enhanced sensitivity to cytokines and are required for T cells to collectively interact.

RESULTS

CDP for CD8+ T cell differentiation

The time course of CD8+ T cell activation in lymph nodes in response to vaccination or infection was characterized by distinct phases of cell motility (**Supplementary Fig. 1a**) and cell-cell interactions[11,12,19] (**Fig. 1a**). To monitor the activity of CD8+ T cells relative to that of APCs during an immune response, we adoptively transferred antigen-specific OT-I T cells (which have transgenic expression of an ovalbumin (OVA)-specific TCR) expressing red fluorescent protein into hosts in which expression of the common DC marker CD11c is marked by yellow fluorescent protein. At 2 h after immunization of mice with a complex of antibody to the DC-specific scavenging molecule DEC-205 linked to OVA (DEC-OVA), which targets DCs as APCs, OT-I T cells intermingled in the antigen-presenting DC network but did not extensively dwell on any single DC (**Supplementary Movie 1**).

[1]Department of Pathology, University of California, San Francisco, San Francisco, California, USA. [2]Division of Rheumatology, Department of Medicine, University of California, San Francisco, San Francisco, California, USA. Correspondence should be addressed to A.G. (audrey.gerard@ucsf.edu) or M.F.K. (matthew.krummel@ucsf.edu).

Received 12 November 2012; accepted 16 January 2013; published online 10 March 2013; doi:10.1038/ni.2547

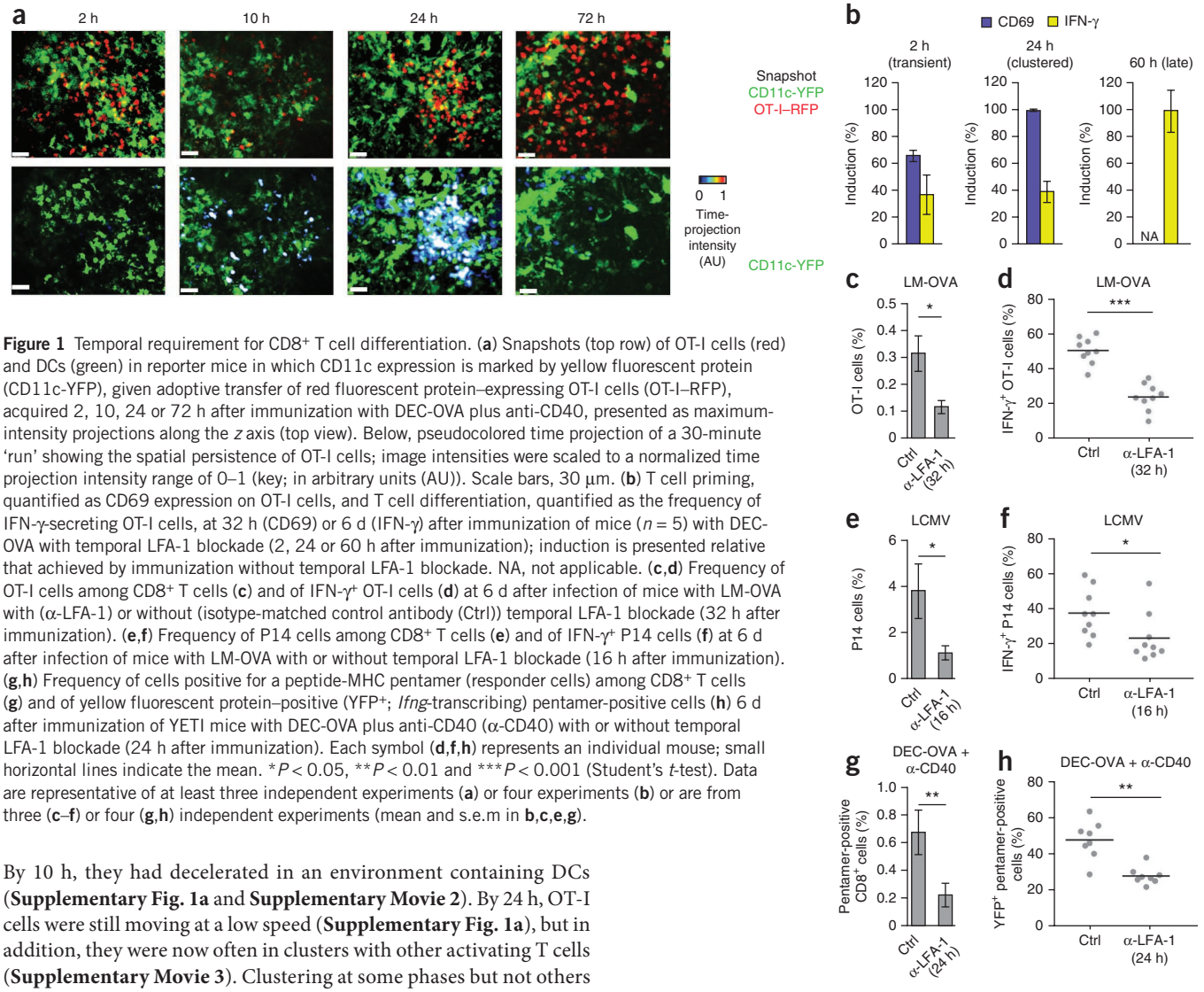

Figure 1 Temporal requirement for CD8⁺ T cell differentiation. (**a**) Snapshots (top row) of OT-I cells (red) and DCs (green) in reporter mice in which CD11c expression is marked by yellow fluorescent protein (CD11c-YFP), given adoptive transfer of red fluorescent protein–expressing OT-I cells (OT-I–RFP), acquired 2, 10, 24 or 72 h after immunization with DEC-OVA plus anti-CD40, presented as maximum-intensity projections along the *z* axis (top view). Below, pseudocolored time projection of a 30-minute 'run' showing the spatial persistence of OT-I cells; image intensities were scaled to a normalized time projection intensity range of 0–1 (key; in arbitrary units (AU)). Scale bars, 30 μm. (**b**) T cell priming, quantified as CD69 expression on OT-I cells, and T cell differentiation, quantified as the frequency of IFN-γ-secreting OT-I cells, at 32 h (CD69) or 6 d (IFN-γ) after immunization of mice ($n = 5$) with DEC-OVA with temporal LFA-1 blockade (2, 24 or 60 h after immunization); induction is presented relative that achieved by immunization without temporal LFA-1 blockade. NA, not applicable. (**c**,**d**) Frequency of OT-I cells among CD8⁺ T cells (**c**) and of IFN-γ⁺ OT-I cells (**d**) at 6 d after infection of mice with LM-OVA with (α-LFA-1) or without (isotype-matched control antibody (Ctrl)) temporal LFA-1 blockade (32 h after immunization). (**e**,**f**) Frequency of P14 cells among CD8⁺ T cells (**e**) and of IFN-γ⁺ P14 cells (**f**) at 6 d after infection of mice with LM-OVA with or without temporal LFA-1 blockade (16 h after immunization). (**g**,**h**) Frequency of cells positive for a peptide-MHC pentamer (responder cells) among CD8⁺ T cells (**g**) and of yellow fluorescent protein–positive (YFP⁺; *Ifng*-transcribing) pentamer-positive cells (**h**) 6 d after immunization of YETI mice with DEC-OVA plus anti-CD40 (α-CD40) with or without temporal LFA-1 blockade (24 h after immunization). Each symbol (**d**,**f**,**h**) represents an individual mouse; small horizontal lines indicate the mean. $*P < 0.05$, $**P < 0.01$ and $***P < 0.001$ (Student's *t*-test). Data are representative of at least three independent experiments (**a**) or four experiments (**b**) or are from three (**c**–**f**) or four (**g**,**h**) independent experiments (mean and s.e.m in **b**,**c**,**e**,**g**).

By 10 h, they had decelerated in an environment containing DCs (**Supplementary Fig. 1a** and **Supplementary Movie 2**). By 24 h, OT-I cells were still moving at a low speed (**Supplementary Fig. 1a**), but in addition, they were now often in clusters with other activating T cells (**Supplementary Movie 3**). Clustering at some phases but not others provides further subcategorization of the characteristics of motility arrest[11]. By 60 h, T cells resumed their migration (**Supplementary Fig. 1a** and **Supplementary Movie 4**). T cell–APC synapses formed in the first hours of DC encounter are known to be sufficient for TCRs to cluster and internalize[20] and for T cells to upregulate expression of the TCR-driven activation marker CD69 (refs. 11,19,20; **Supplementary Fig. 1b**).

To address the requirement for adhesive synaptic contacts throughout the time course of the response, we injected antibody to the integrin LFA-1 (anti-LFA-1) into mice to block those interactions. We initiated this blockade at times corresponding to the transient (2 h), clustered (24 h) and very late (60 h) time points[11,12,19] (**Fig. 1b**). Anti-LFA-1 administered 2 h after antigen administration diminished proximal upregulation of CD69 expression at 32 h by ~30% and the extent of T cell differentiation, exemplified by production of interferon-γ (IFN-γ), at day 6 by ~60% (**Fig. 1b** and **Supplementary Fig. 1b**,**c**). That result was consistent with broad facilitation of both priming and differentiation by adhesive synapses. In contrast, blockade of LFA-1 that began at 24 h had no effect on CD69 expression at any subsequent time (**Fig. 1b** and **Supplementary Fig. 1b**) or on proliferation (**Supplementary Fig. 1d**). However, that 24-hour blockade resulted in ~60% less induction of IFN-γ production in OT-I cells than that in OT-I cells from mice that received control antibody by day 6 (**Fig. 1b** and **Supplementary Fig. 1b**), suggestive of a different requirement for differentiation than for priming. Because of experimental constraints, we adoptively transferred 1×10^6 OT-I T cells into wild-type recipient mice for early assessment of the upregulation of CD69 expression at 32 h, as that number of cells is needed to for sufficient recovery of cells, but we adoptively transferred only 5×10^3 OT-I T cells to measure IFN-γ expression, as that number of cells is more physiologically accurate[21,22]. We confirmed that differentiation still required LFA-1-dependent interactions at 24 h after immunization with a higher frequency of precursor cells, although nonphysiological frequency of precursor cells alone resulted in more differentiation regardless of blockade (**Supplementary Fig. 1e**). Blocking LFA-1-dependent interactions 60 h after immunization had no effect on IFN-γ production (**Fig. 1b** and **Supplementary Fig. 1c**), which suggested there was a short time window (24–60 h) during which T cells integrated differentiation cues in a cell contact–dependent manner.

We obtained similar evidence of a requirement for integrin through the use of a different adjuvant-immunization model with delayed blockade of ICAM-1, the ligand for LFA-1 (**Supplementary Fig. 2**). This indicated that inhibition of differentiation was not due to anti-LFA-1-modulated signaling or blockade of T cell trafficking. Finally, because treatment with anti-LFA-1 could function by blocking the late entry of new OT-I cells into lymph nodes and thus potentially affect

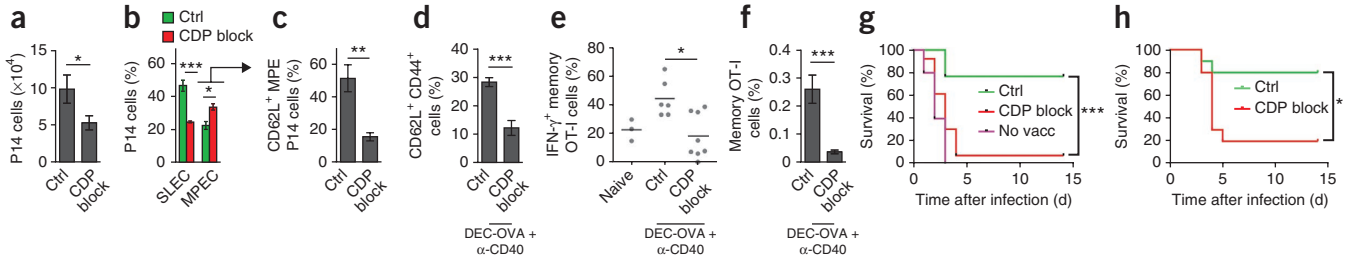

Figure 2 The generation of central memory precursor cells and the recall response depends on LFA-1-dependent stable interactions during the CDP. (**a**–**c**) Total P14 cells (**a**) and expression of the surface markers KLRGI and IL7R by P14 cells (**b**) and of CD62L by P14 memory precursor effector cells from **b** (arrow; **c**) in mice ($n = 6$) given adoptive transfer of 5×10^3 P14 cells and then infected with LCMV with (CDP block) or without (Ctrl) CDP blockade, assessed 15 d after immunization. SLEC, short-lived effector cells ($KLRGI^{hi}IL\text{-}7R^{lo}$ P14 cells); MPEC, memory precursor effector cells ($KLRGI^{lo}IL\text{-}7R^{hi}$ P14 cells). (**d**) Frequency of $CD62L^+CD44^+$ cells among OT-I cells in mice given adoptive transfer of 5×10^3 OT-I cells and immunized with DEC-OVA plus anti-CD40 with or without CDP blockade, assessed 8 d after immunization. (**e**,**f**) Frequency of IFN-γ-secreting OT-I cells (**e**) and of OT-I cells among $CD8^+$ T cells (**f**) after recall 30 d after immunization as in **d**. Naive (**e**), mice given adoptive transfer of OT-I cells but not immunized. Each symbol (**e**) represents an individual mouse; small horizontal lines indicate the mean. (**g**) Survival of mice ($n = 13$) given adoptive transfer of 5×10^3 OT-I cells and left unvaccinated (No vacc) or vaccinated with OVA peptide–pulsed DCs with or without CDP blockade, then challenged with a lethal dose of LM-OVA (2× to 10× the half-maximal lethal dose (LD_{50})) at 40–60 d after vaccination. (**h**) Survival of recipient mice ($n = 10$) treated as follows: donor mice were given adoptive transfer and vaccinated as in **g**, followed by isolation of OT-I cells 6 d after immunization and transfer of 5×10^3 cells into naive recipient mice that were then challenged with a lethal dose of LM-OVA (2× the LD_{50}) 70 d after transfer. $^*P < 0.05$, $^{**}P < 0.01$ and $^{***}P < 0.001$ (Student's *t*-test (**a**,**c**,**d**,**f**), two-way (**b**) or one-way (**e**) analysis of variance (ANOVA) or Mantel-Cox test (**g**,**h**)). Data are from three (**a**–**f**) or two (**g**,**h**) independent experiments (mean and s.e.m. in **a**–**f**).

memory through the activation of different cells, we synchronized the homing of T cells to lymph nodes by treating the mice with antibody to the lymph node–homing receptor CD62L to block new entry[23]. Treatment with anti-CD62L did not affect IFN-γ production by OT-I cells, and treatment with anti-LFA-1 in the context of CD62L blockade still resulted in inhibition of IFN-γ production (**Supplementary Fig. 1f**). That result confirmed that inhibition of $CD8^+$ T cell differentiation by treatment with anti-LFA-1 was not due to inhibition of T cell homing or inhibition of late T cell–APC encounters.

We also observed a similarly lower yield and number of antigen-specific effector $CD8^+$ T cells and proportion of IFN-γ^+ antigen-specific cells in mice treated with anti-LFA-1 than in mice treated with isotype-matched control antibody in response to sublethal infection with bacteria (OVA-expressing *Listeria monocytogenes* (LM-OVA); **Fig. 1c**,**d** and **Supplementary Fig. 3c**) or virus (lymphocytic choriomeningitis virus (LCMV); **Fig. 1e**,**f** and **Supplementary Fig. 3d**). For these experiments, we adjusted the timing of the treatment with anti-LFA-1 to the time when markers of TCR-driven activation were maximal; that is, at 32 h or 16 h for infection with LM-OVA or LCMV, respectively (**Supplementary Fig. 3a**,**b**). Finally, we observed a similar requirement for secondary adhesive contacts when a we assayed responder mouse without transgenic TCR expression (the YETI mouse), using pentamers of peptide and major histocompatibility complex (MHC) to identify responder $CD8^+$ T cells in the endogenous repertoire and using yellow fluorescent protein as a 'readout' of *Ifng* transcription (**Fig. 1g**,**h** and **Supplementary Fig. 3e**). These data provided evidence of a late requirement for integrin-mediated interactions during a variety of immunological challenges and at physiological frequencies of precursor cells.

CDP interactions mediate protective memory

As these data reported above indicated a distinct CDP (24–48 h after immunization) for integrin-mediated engagements, we also tested the consequences of blocking LFA-1-dependent interactions during the CDP (called 'CDP blockade' here) on the establishment of memory and successful vaccination. We adoptively transferred a small number of P14 T cells (with transgenic expression of a TCR specific for amino acids 33–41 of LCMV glycoprotein) into wild-type hosts and found that during infection of those hosts with LCMV, CDP blockade resulted in fewer P14 cells 2 weeks after challenge (**Fig. 2a**). Furthermore, the balance between short-lived effector cells and memory precursor effector cells was altered by CDP blockade (**Fig. 2b**). Blocking LFA-1-dependent interactions during the CDP led to a lower frequency of short-lived effector cells and, conversely, more memory precursor effector cells at day 15 after infection. However, of those memory precursor effector cells, the frequency with a central memory phenotype was much lower (**Fig. 2c**), which suggested that the establishment of long-lasting memory was impaired. That observation held true for CDP blockade after immunization with DEC-OVA, which resulted in a lower frequency of OT-I cells with central memory phenotype, as assessed by a $CD62L^+$ and $CD44^+$ phenotype at day 8 (28.37% for mice treated with control antibody and 12.28% for mice treated with anti-LFA-1; **Fig. 2d**). As a consequence of that blockade, we also found fewer IFN-γ-producing cells among the cells recovered 3 d after recall experiments (**Fig. 2e**), as well as a lower frequency of recovered OT-I cells (**Fig. 2f**). These data suggested that successful vaccination would rely on the CDP. We modified an established DC-vaccination protocol against LM-OVA[24] and blocked LFA-1-dependent interactions during the CDP to establish the relevance of this period for protection. Normal vaccination conferred protection against a lethal dose of LM-OVA on 80% of mice, whereas those vaccinated under conditions of CDP blockade showed just 5% survival (**Fig. 2g**).

Finally, we sought to understand whether the failure of DC vaccination was caused only by a lower total cell number or also by an actual defect in differentiation due to CDP blockade. We adoptively transferred a small number of OT-I cells into two sets of recipient mice and either blocked or did not block LFA-1-dependent interactions during the CDP. We then isolated OT-I cells from those mice 6 d after DC vaccination with or without CDP blockade and transferred equal numbers of OT-I cells into cohorts of naive recipients to allow those to establish memory. We then challenged recipient mice with a lethal dose of LM-OVA at least 70 d after transfer. OT-I cells generated from DC vaccination in the context of CDP blockade were unable to effectively protect mice, in contrast to cells that arose from vaccination without CDP blockade (**Fig. 2h**). In summary, we concluded that not only cell number but also cell differentiation were regulated during the CDP and were necessary for optimal DC vaccination.

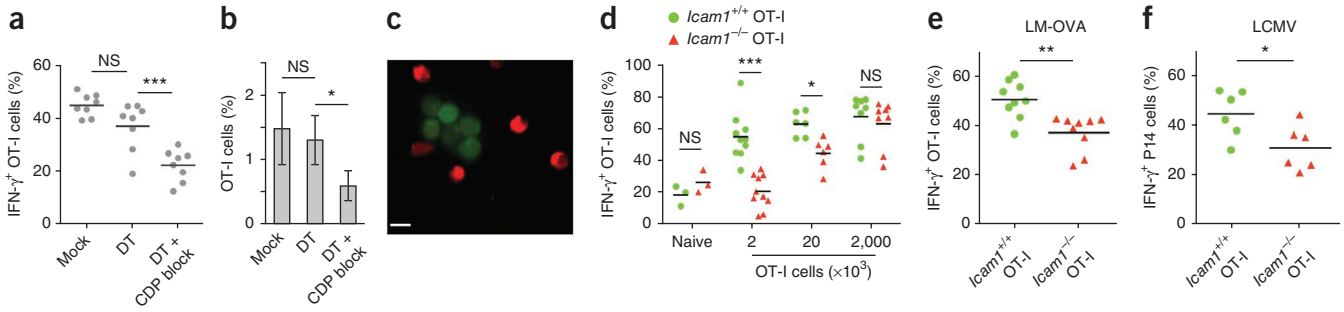

Figure 3 CD8+ T cell differentiation relies mainly on T cell–T cell contacts. (**a**,**b**) Frequency of IFN-γ-secreting OT-I cells (**a**) and of OT-I cells among CD8+ T cells (**b**) in H-2K^{bm1} mice bearing H-2K^{bm1} OT-I cells, immunized with OVA peptide–pulsed BMDCs generated from CD11c-DTR mice, followed by mock treatment (Mock) or ablation of APCs with diphtheria toxin alone (DT) or with CDP blockade (DT + CDP block), analyzed at the peak of the effector response. (**c**) Microscopy of clusters of an admixture of 1 x 10^6 fluorescence-labeled *Icam1*$^{+/+}$ (green) and *Icam1*$^{-/-}$ (red) T cells 24 h after activation with the phorbol ester PMA and ionomycin. Scale bar, 5 μm. (**d**) Effector response of *Icam1*$^{+/+}$ and *Icam1*$^{-/-}$ OT-I cells before (Naive) and 6 d after immunization with DEC-OVA, quantified as the frequency of IFN-γ-secreting OT-I cells. (**e**) Effector response of *Icam1*$^{+/+}$ and *Icam1*$^{-/-}$ OT-I cells 8 d after immunization with LM-OVA, quantified as in **e**. (**f**) Effector response of *Icam1*$^{+/+}$ and *Icam1*$^{-/-}$ P14 cells 8 d after immunization with LCMV, quantified as the frequency of IFN-γ-secreting P14 cells. Each symbol (**a**,**d**–**f**) represents an individual mouse; small horizontal lines indicate the mean. NS, not significant, $*P < 0.05$, $**P < 0.01$ and $***P < 0.001$ (one-way (**a**,**b**) or two-way (**d**) ANOVA, or Student's *t*-test (**e**,**f**)). Data are from at least three independent experiments (**a**,**b**; mean and s.e.m. in **b**) or are from three independent experiments (**d**–**f**).

Function of cell interactions beyond T cell–APC

The synaptic requirement for LFA-1 on T cells has been linked to stabilized binding to antigen-presenting DCs bearing the counter-ligand ICAM-1 (ref. 25). We therefore sought to formally investigate the requirement for DCs as the synaptic partners of T cells during the CDP. To do so, we immunized mice with a pure population of antigen-pulsed bone marrow–derived DCs (BMDCs) generated from CD11c-DTR mice, which are transiently depleted of CD11c+ cells after the administration of diphtheria toxin[26]. We injected diphtheria toxin into these mice in such a way that the adopted APCs were fully ablated by the start of the CDP without affecting earlier T cell priming (**Supplementary Fig. 4**). Both host and responding OT-I T cells in our study were homozygous for the variant H-2K^{bm1} allele, which rendered them unable to present peptides on their own MHC molecules to the OT-I cells. Ablation of APCs, which was complete by 24 h after immunization (**Supplementary Fig. 4**), did not significantly affect IFN-γ production by OT-I cells (**Fig. 3a**) or their population expansion (**Fig. 3b**). However, CDP blockade at 24 h after immunization in the context of APC ablation significantly inhibited both measures (**Fig. 3a**,**b**). Published studies have established that prolonged interaction with APCs does not control the functionality of the CD8+ T cell response *in vitro*[27–29] or *in vivo*[30] but have suggested that T cell differentiation is cell autonomous after APC encounter. Our data confirmed those published findings but suggested that the differentiation cue during the CDP was in fact reliant on an adhesive interaction with another cell or surface.

T cells use LFA-1 to form homotypic 'clusters', creating a relatively transient T cell–T cell synapse[9,31]. That interaction required T cells that bore ICAM-1 (**Fig. 3c** and **Supplementary Fig. 5a**,**b**). However, ICAM-1 expression on T cells was not necessary for T cell–APC interactions, as *Icam1*$^{-/-}$ OT-I T cells were at least as proficient as *Icam1*$^{+/+}$ OT-I T cells in forming stable interactions with antigen-bearing DCs (**Supplementary Fig. 5c**). We assessed the requirement for ICAM-1 on T cells in effector differentiation by adoptively transferring various numbers of allelically marked *Icam1*$^{+/+}$ OT-I T cells and *Icam1*$^{-/-}$ OT-I T cells into the same (wild-type) host and measuring the frequency of IFN-γ-expressing cells 6 d after immunization with DEC-OVA (**Fig. 3d**). The differentiation of *Icam1*$^{-/-}$ OT-I T cells was impaired relative to that of control *Icam1*$^{+/+}$ OT-I cells when we transferred 1 × 10^3 cells of each genotype. Larger numbers of transferred cells 'rescued' the inhibition of CD8+ T cell differentiation induced by ICAM-1 deficiency. Given those results, we concluded that there was a requirement for T cells to be bound by other cells, probably other T cells, especially when physiologically relevant numbers of T cells were activating. Expression of full-length ICAM-1 on CD8+ T cells was similarly required for an optimal CD8+ T cell response to LM-OVA (**Fig. 3e**) or LCMV (**Fig. 3f**). Mice given adoptive transfer of small numbers of *Icam1*$^{-/-}$ OT-I T cells were also less protected by vaccination for protection against a lethal dose of LM-OVA than were mice bearing the same number of *Icam1*$^{+/+}$ OT-I T cells (**Supplementary Fig. 5d**). From these experiments, we concluded that ICAM-1 expression on T cells, and therefore cell interactions beyond those mediated by APCs, were formative for CD8+ T cell differentiation in response to immunization.

T cell–T cell interactions are autonomous but facilitated by APCs

The findings reported above led us to consider T cells themselves an alternative LFA-1-bearing partner during the CDP, so we examined the dynamics of T cell interactions centered on the CDP in the presence or absence of ICAM-1 on T cells. We turned to two-photon microscopy of lymph nodes with *Icam1*$^{+/+}$ or *Icam1*$^{-/-}$ OT-I cells labeled with distinct dyes, and adoptively transferred 2 × 10^6 cells to facilitate statistical analysis. In time projections of T cell zones, *Icam1*$^{-/-}$ OT-I T cells were less stable in their positions at 24 h than were their *Icam1*$^{+/+}$ counterparts, but these cells were in the same T cell compartments (**Fig. 4a** and **Supplementary Fig. 6a**). Furthermore, *Icam1*$^{-/-}$ OT-I T cells typically left clusters more quickly than did their *Icam1*$^{+/+}$ counterparts, either when those clusters contained only *Icam1*$^{-/-}$ OT-I cells or were a mixture of *Icam1*$^{+/+}$ and *Icam1*$^{-/-}$ OT-I cells (**Fig. 4b** and **Supplementary Movie 5**). Those findings suggested that T cells must be able to be bound to optimize arrest adjacent to other T cells. CDP blockade with anti-LFA-1 also resulted in a lower frequency (approximately 50%) of OT-I cells in T cell–T cell clusters within 2 h of blockade (**Fig. 4c** and **Supplementary Movies 3** and **6**), which showed that T cell–T cell interactions were inhibited similarly by blockade of either LFA-1 or its ligand.

ICAM-1 on T cells was thus required for stabilization of the T cell position adjacent to other T cells during the deceleration phase.

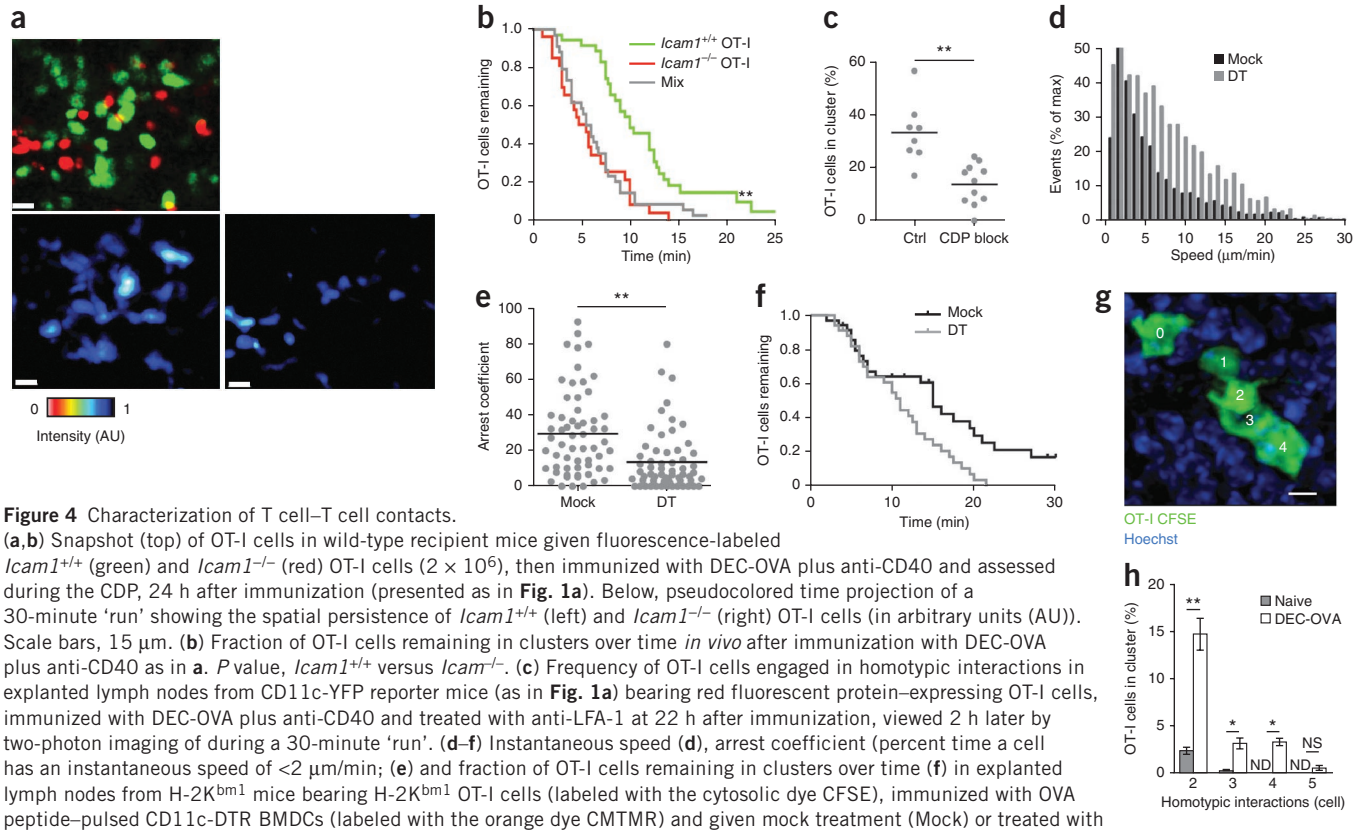

Figure 4 Characterization of T cell–T cell contacts. (**a**,**b**) Snapshot (top) of OT-I cells in wild-type recipient mice given fluorescence-labeled *Icam1*$^{+/+}$ (green) and *Icam1*$^{-/-}$ (red) OT-I cells (2×10^6), then immunized with DEC-OVA plus anti-CD40 and assessed during the CDP, 24 h after immunization (presented as in **Fig. 1a**). Below, pseudocolored time projection of a 30-minute 'run' showing the spatial persistence of *Icam1*$^{+/+}$ (left) and *Icam1*$^{-/-}$ (right) OT-I cells (in arbitrary units (AU)). Scale bars, 15 μm. (**b**) Fraction of OT-I cells remaining in clusters over time *in vivo* after immunization with DEC-OVA plus anti-CD40 as in **a**. *P* value, *Icam1*$^{+/+}$ versus *Icam*$^{-/-}$. (**c**) Frequency of OT-I cells engaged in homotypic interactions in explanted lymph nodes from CD11c-YFP reporter mice (as in **Fig. 1a**) bearing red fluorescent protein–expressing OT-I cells, immunized with DEC-OVA plus anti-CD40 and treated with anti-LFA-1 at 22 h after immunization, viewed 2 h later by two-photon imaging of during a 30-minute 'run'. (**d**–**f**) Instantaneous speed (**d**), arrest coefficient (percent time a cell has an instantaneous speed of <2 μm/min; (**e**) and fraction of OT-I cells remaining in clusters over time (**f**) in explanted lymph nodes from H-2K^{bm1} mice bearing H-2K^{bm1} OT-I cells (labeled with the cytosolic dye CFSE), immunized with OVA peptide–pulsed CD11c-DTR BMDCs (labeled with the orange dye CMTMR) and given mock treatment (Mock) or treated with diphtheria toxin (DT) 8 h later and analyzed by two-photon imaging 24–30 h after immunization, during the CDP. (**g**) Cluster of four OT-I cells (1–4) and an isolated cell (0) present during the CDP after immunization with DEC-OVA plus anti-CD40 and transfer of a low frequency (1×10^4) of precursor OT-I cells, presented as a maximum-intensity projection along the *z* axis (top view). (**h**) Frequency of OT-I cell clusters in whole popliteal lymph nodes from naive or DEC-OVA-immunized wild-type mice given a low frequency of precursor cells ($n = 338$ (naive) or 320 (DEC-OVA)). ND, not detected. Each symbol represents an individual field (**c**) or cell (**e**); horizontal lines indicate the mean. $^*P < 0.05$ and $^{**}P < 0.001$ (Mantel-Cox test (**b**), Student's *t*-test (**c**,**d**) or two-way ANOVA (**h**)). Data are from two (**a**,**b**,**g**), four (**c**,**d**–**f**) or three (**h**) independent experiments (mean and s.e.m. in **h**).

Consistent with the fact that APCs are the main 'nucleator' of decelerated T cells, OT-I T cells moved faster and arrested for a shorter period when APCs were ablated during the CDP (**Fig. 4d**,**e** and **Supplementary Movies 7** and **8**). Under those conditions, T cell–T cell contacts were similarly stable over the first ~10 min, although T cells were then more weakly associated over longer times (**Fig. 4f** and **Supplementary Movies 7** and **8**). A similar lifetime of association has been observed for CD4$^+$ T cell–CD4$^+$ T cell synapses[9]. Together these results indicated that arrest and interaction was a 'milieu effect' driven both by APCs and by lateral homotypic interactions.

A secondary, 'collective' phase of cellular programming, during which primed T cells mingle, would require T cell–T cell interactions to be not only avid but also sufficiently frequent, particularly when the number of primed cells are limited. By surveying entire lymph nodes 24 h after immunization, we found that T cell–T cell contacts were selected for and occurred when precursors were introduced at physiological frequencies (**Fig. 4g** and **Supplementary Fig. 6b**). Quantification of the recovered cells in lymph nodes demonstrated a greater frequency of clusters containing two, three or four cells at this time, an effect that was immunization dependent (**Fig. 4h**). That confirmed the proposal that close T cell–T cell contacts were a feature of priming, even with a low frequency of precursor cells. Although the mechanism for promoting the interaction may simply involve ongoing random migration and selective adhesion, it is also possible that such interactions profit from early chemokines for cells to find each other at dynamically selected sites in the entire volume of the lymph node[7,8].

T cell interactions promote critical synaptic cytokine exchange

T cell differentiation is driven mainly by cytokines, and these can be directed into both T cell–APC synapses and T cell–T cell synapses[9,32]. CD8$^+$ T cells began to make IFN-γ within 24 h of immunization of wild-type mice with DEC-OVA[33] (**Supplementary Fig. 7a**). By expressing IFN-γ fused to green fluorescent protein (IFN-γ–GFP) in T cell blasts and tracking T cell–T cell contacts, we observed that vesicles containing IFN-γ were recruited to the site of contact (**Fig. 5a**,**b** and **Supplementary Movie 9**). Furthermore, T cells participating in clusters in the absence of APCs *in vitro* indeed secreted IFN-γ (**Fig. 5c**), and they did so 'preferentially' inward toward each other (**Fig. 5d**). IFN-γ was secreted at sites of T cell–T cell contacts at which we also found enrichment for ICAM-1 (**Supplementary Fig. 7b** and **Supplementary Movie 10**), which demonstrated the existence of an immunological synapse between CD8$^+$ T cells. Intracellular IFN-γ was directed between adjacent T cells *in vivo* during the CDP after immunization with DEC-OVA (**Fig. 5e**). To investigate the function of the secretion of IFN-γ from one T cell to another, we primed T cells in the absence of APCs with pharmacological mimics of TCR signaling and blocked synaptic interaction through the use of anti-LFA1, in the presence or absence of exogenous IFN-γ or blockade of IFN-γ. We then transferred those cells into wild-type mice and assayed a recall response approximately 30 d later (**Supplementary Fig. 7c**). Blockade of either LFA-1 or IFN-γ in the first day of APC-free stimulation resulted in a lower frequency of IFN-γ$^+$ cells after recall (**Fig. 5f**). In this assay, *in vitro* treatment with anti-LFA-1 also

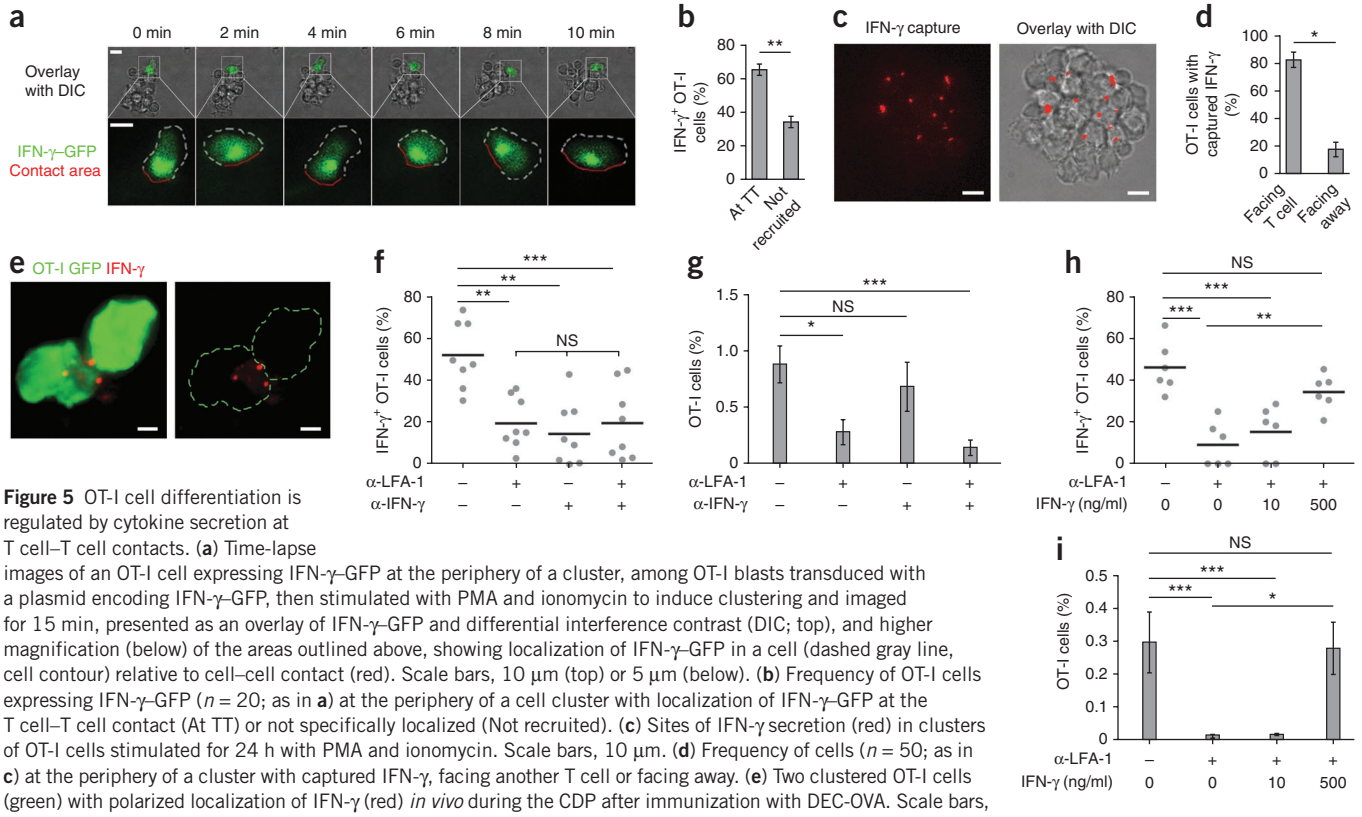

Figure 5 OT-I cell differentiation is regulated by cytokine secretion at T cell–T cell contacts. (**a**) Time-lapse images of an OT-I cell expressing IFN-γ–GFP at the periphery of a cluster, among OT-I blasts transduced with a plasmid encoding IFN-γ–GFP, then stimulated with PMA and ionomycin to induce clustering and imaged for 15 min, presented as an overlay of IFN-γ–GFP and differential interference contrast (DIC; top), and higher magnification (below) of the areas outlined above, showing localization of IFN-γ–GFP in a cell (dashed gray line, cell contour) relative to cell–cell contact (red). Scale bars, 10 μm (top) or 5 μm (below). (**b**) Frequency of OT-I cells expressing IFN-γ–GFP ($n = 20$; as in **a**) at the periphery of a cell cluster with localization of IFN-γ–GFP at the T cell–T cell contact (At TT) or not specifically localized (Not recruited). (**c**) Sites of IFN-γ secretion (red) in clusters of OT-I cells stimulated for 24 h with PMA and ionomycin. Scale bars, 10 μm. (**d**) Frequency of cells ($n = 50$; as in **c**) at the periphery of a cluster with captured IFN-γ, facing another T cell or facing away. (**e**) Two clustered OT-I cells (green) with polarized localization of IFN-γ (red) *in vivo* during the CDP after immunization with DEC-OVA. Scale bars, 5 μm. (**f**,**g**) Frequency of IFN-γ-secreting OT-I cells (**f**) and of OT-I cells among CD8$^+$ T cells (**g**) from wild-type mice given OT-I cells activated *in vitro* with PMA and ionomycin and left untreated (–) or treated (+) with anti-LFA-1 and/or anti-IFN-γ (below graphs) and transferred 3 d later, analyzed after *in vivo* recall. (**h**,**i**) Frequency of IFN-γ-secreting OT-I cells (**h**) and of OT-I cells among CD8$^+$ T cells (**i**) from wild-type mice given OT-I cells activated as in **f**,**g** and left untreated (–) or treated (+) with anti-LFA-1 and various concentrations of IFN-γ (below graphs) and transferred 3 d later, analyzed after *in vivo* recall. $^*P < 0.05$, $^{**}P < 0.01$ and $^{***}P < 0.001$ (Student's *t*-test (**b**,**d**) or one-way ANOVA (**f**–**i**)). Data are representative of two experiments (**a**,**b**) or are from three independent experiments (**c**,**d**,**f**–**i**) (mean and s.e.m.).

blocked the overall recovery of T cells, but treatment with anti-IFN-γ did not; this may have been an effect on homing back into lymph nodes or may have reflected the requirement for other signals delivered at T cell–T cell contacts (**Fig. 5g**). The addition of IFN-γ back into this assay resulted in a dose-dependent recovery of IFN-γ production by differentiated cells after recall (**Fig. 5h**), consistent with the proposal that this signaling axis was sufficient as well as necessary for differentiation. However, full restoration in the presence of anti-LFA-1 required 50 times more IFN-γ than the concentration typically used to skew differentiation when the T cell–T cell contact was untouched (data not shown). For reasons that are unclear at present, very high IFN-γ doses also restored the number of cells recovered (**Fig. 5i**), even in the presence of anti-LFA-1. The IFN-γ receptor CD119 was also required for CD8$^+$ T cells at physiological frequencies of precursor cells to commit to producing IFN-γ *in vivo* (**Supplementary Fig. 7d–g**). Given these results, we concluded that IFN-γ shared through T cell–T cell synapses contributed to CD8$^+$ T cell differentiation.

DISCUSSION

Our results here have provided evidence of a second stage of information exchange through cell-cell communication that is necessary for an effective immune response. We propose that during motility arrest, prolonged juxtaposition to APCs in the T cell zone also facilitates other types of cell-cell synaptic communication, including T cell–T cell synapses, which enhance collective differentiation. A collective phase may involve additional cell types beyond T cells that join clusters and may also involve additional cytokines beyond those studied here.

Although it has been proposed that the arrest phase mediates mainly key interactions with APCs, published evidence suggests that such prolonged interaction with APCs does not control the functionality of CD8$^+$ T cell responses *in vitro*[27–29] or *in vivo*[30]. Consistent with the proposal that antigen presentation is most relevant only at an early time, we did not observe inhibition of the upregulation of CD69 expression or proliferation when cell-cell interactions were blocked during the CDP. Motility arrest in the T cell zone therefore seems to have functions other than TCR triggering. Specifically, T cell–T cell contacts during the CDP regulated the balance between effector and memory cells but also potentiated the amplification and/or survival of CD8$^+$ T cells. Blockade at 24 h resulted in apparent defects as early as day 6 and resulted in profoundly poor protection in the late phase. Analysis of markers showed that the early defects corresponded to an early failure to commit to central memory cells, which are critical for lasting protection[34].

We found clustering of T cells after immunization when we used physiological frequencies of precursor cells. But how do rare T cells converge on particular sites in the lymph node? There is evidence that DCs produce the chemokines CCL3 and CCL4, which attract CD8$^+$ T cells expressing the chemokine receptor CCR5, in a CD4$^+$ T cell–dependent manner, and it has been proposed that this phenomenon guides antigen-specific CD8$^+$ T cells to DCs for priming[7]. APCs, especially those that have been helped by CD4$^+$ T cells, would produce such chemokines and assist in attracting experienced CD8$^+$ T cells and bringing them together. This scenario may underlie the effective functioning of T cell–T cell interactions at a low frequency of

precursor cells, and in this scenario, clustering and the ensuing 'collective' differentiation would be a consequence of help from T cells.

T cell–T cell interactions are not recognized as being involved in end-point assays, although the formation of T cell clusters after T cell activation has been documented as a nucleation around APCs and has been observed as a 'read-out' of strong T cell activation[9,12,15–17]. Here we have provided evidence that CD8$^+$ T cells obtained information not only from the APC but also from the other T cells in such clusters, both *in vitro* and *in vivo*. The exchange of information between CD8$^+$ T cells required integrin-mediated contact and the formation of a T cell–T cell synapse. Although T cell–T cell synapses and cytokine sharing have been already described for CD4$^+$ T cells *in vitro*[9], we have now demonstrated that CD8$^+$ T cells also shared cytokines, including IFN-γ, *in vitro* as well as *in vivo*, and, more notably, that T cell–T cell communication was a relevant facilitator of the downstream 'output': T cell differentiation. T cell differentiation resulting from T cell–T cell adhesive 'secondary' synapses provides a platform that is an alternative to the immunological synapse for very local cytokine exchange. Such contact might also provide a platform other than the APC to facilitate asymmetric cell division[35].

Although it is well established that IFN-γ is crucial for T helper type 1 differentiation[36], our results suggest that its importance for CD8$^+$ T cell differentiation has been underestimated so far. One reason for this could be the frequency of antigen-specific CD8$^+$ T cells used in previously published studies, which we found was important, as other signals seemed to be sufficient in our studies when we used an overly large number of antigen-specific CD8$^+$ T cells. We speculate that in response to stimuli beyond those tested in our study, IFN-γ may also have a different effect on T cells, perhaps through its production or action on additional partners[37]. Although some cytokines in some responses are certainly dispersed globally[9,38], secondary synapses and localized synapses provide specificity as well as amplification, probably even under those conditions. Finally, our work suggests careful exploration of the aggregation of cytokine receptors in synapses, as blockade of LFA-1 resulted in less sensitivity to cytokines delivered at T cell–T cell contacts. Indeed, the expression and activity of the receptor for IFN-γ is regulated after *in vitro* stimulation or immunization of mice with LM-OVA[39,40], and this may actually lead to heightened selection for cytokines delivered by cell-cell contact.

Our data suggest that T cell–T cell contacts enhance the population expansion and differentiation of CD8$^+$ T cells. However, we propose that direct communication between T cells allows them to collectively respond and control the size of the effector and memory pool. This indicates that whereas some cells would be rescued or amplified, others would be deleted. This could be true especially for a polyclonal response, and T cell clusters would be more typically composed of heterogeneous T cells that influence each other's fate. This would explain how heterogeneous T cell populations respond in a coordinated manner.

T cell–T cell synapses may also facilitate and underlie the exchange of information other than cytokines. For example, T cells have been shown in some experiments to capture peptide-MHC complexes and mediate antigen-specific signaling to other CD8$^+$ T cells[41]. Similarly, antigen-specific CD4$^+$ T cell–CD4$^+$ T cell interactions may regulate population expansion after upregulation of MHC class II expression in CD4$^+$ T cells[42]. Finally, a published study has suggested cells that upregulate the Hippo pathway, which is known to link cell-cell contact to differentiation in other cell lineages, may commit cells to terminal effector differentiation[43], and the synapse process we have characterized here may provide a framework for the delivery of such signals.

Collective activity typically arises when a collection of organisms or cells coordinate their responses. For example, colonies of bees make a collective decision to select the best nectar source not by having each bee visit all sources but by having bees visit different sources, followed by later comparisons at the hive[44]. At a cellular level, in collective germ-cell migration, each cell can move in the cluster and function somewhat autonomously, but the collection of cells migrates toward a stimulus[45]. Similar activity has been observed during cancer metastasis, in which cooperation between invasive and noninvasive cells enables the extravasation of otherwise nonmetastatic cells[46]. Collective decision-making is thus a collection of stochastic events that, through positive reinforcement, allows the individual components to select the optimal response for the system. The immune system may represent a new twist on this, as it uses the rather transient formation of synapses between many cell types to achieve the goal of collective decisions. The formation of T cell–T cell synapses would seem in this context to provide a feedback system for the comparison and selection of an effector-memory response dictated by the experiences of other individual activated T cells. Notably, such interactions, hours after critical T cell–APC interactions initiate T cell activation, may provide feedback that regulates many other facets of the response, including system-wide tolerance. More broadly, immunological synapses between many different types of cells of the immune system, not just between T cells and APCs, may represent a critical mechanism for enhancing collective decision-making and, at the same time, for limiting the exposure of adjacent cells to effector signals. Our work thus establishes a framework for considering synapses as mediators that integrate information across many concurrently activating cells and generate concerted immune responses.

METHODS

Methods and any associated references are available in the online version of the paper.

Note: Supplementary information is available in the online version of the paper.

ACKNOWLEDGMENTS

We thank M. Nussenzeig (Rockefeller University) for CD11c-YFP mice; M. Coles (Medial Research Council, York) for CD2-RFP mice; R. Locksley (University of California at San Francisco) for YETI mice; and personnel of the Biological Imaging Development Center for technical assistance with imaging. Supported by the Juvenile Diabetes Foundation (M.F.K.) and the US National Institutes of Health (R01AI52116 to M.F.K.).

AUTHOR CONTRIBUTIONS

A.G. and M.F.K. designed the experiments and wrote and revised the manuscript; A.G. did the experiments; O.K. did or participated in experiments involving immunization with LCMV and LM-OVA; P.B. analyzed data and generated Matlab scripts; E.O. generated IFN-γ–GFP constructs and did preliminary experiments; and J.H. and M.M. provided P14 mice and participated in LCMV-challenge experiments.

COMPETING FINANCIAL INTERESTS

The authors declare no competing financial interests.

1. Lefrançois, L. & Obar, J.J. Once a killer, always a killer: from cytotoxic T cell to memory cell. *Immunol. Rev.* **235**, 206–218 (2010).
2. Pipkin, M.E. *et al.* Interleukin-2 and inflammation induce distinct transcriptional programs that promote the differentiation of effector cytolytic T cells. *Immunity* **32**, 79–90 (2010).
3. Prlic, M., Williams, M.A. & Bevan, M.J. Requirements for CD8 T-cell priming, memory generation and maintenance. *Curr. Opin. Immunol.* **19**, 315–319 (2007).
4. Mescher, M.F. *et al.* Signals required for programming effector and memory development by CD8$^+$ T cells. *Immunol. Rev.* **211**, 81–92 (2006).
5. Obar, J.J. & Lefrancois, L. Early events governing memory CD8$^+$ T-cell differentiation. *Int. Immunol.* **22**, 619–625 (2010).

6. Kaech, S.M. & Wherry, E.J. Heterogeneity and cell-fate decisions in effector and memory CD8+ T cell differentiation during viral infection. *Immunity* **27**, 393–405 (2007).
7. Castellino, F. *et al.* Chemokines enhance immunity by guiding naive CD8+ T cells to sites of CD4+ T cell-dendritic cell interaction. *Nature* **440**, 890–895 (2006).
8. Hugues, S. *et al.* Dynamic imaging of chemokine-dependent CD8+ T cell help for CD8+ T cell responses. *Nat. Immunol.* **8**, 921–930 (2007).
9. Sabatos, C.A. *et al.* A synaptic basis for paracrine interleukin-2 signaling during homotypic T cell interaction. *Immunity* **29**, 238–248 (2008).
10. Foulds, K.E. & Shen, H. Clonal competition inhibits the proliferation and differentiation of adoptively transferred TCR transgenic CD4 T cells in response to infection. *J. Immunol.* **176**, 3037–3043 (2006).
11. Mempel, T.R., Henrickson, S.E. & Von Andrian, U.H. T-cell priming by dendritic cells in lymph nodes occurs in three distinct phases. *Nature* **427**, 154–159 (2004).
12. Miller, M.J., Safrina, O., Parker, I. & Cahalan, M.D. Imaging the single cell dynamics of CD4+ T cell activation by dendritic cells in lymph nodes. *J. Exp. Med.* **200**, 847–856 (2004).
13. Miller, M.J., Wei, S.H., Parker, I. & Cahalan, M.D. Two-photon imaging of lymphocyte motility and antigen response in intact lymph node. *Science* **296**, 1869–1873 (2002).
14. Stoll, S., Delon, J., Brotz, T.M. & Germain, R.N. Dynamic imaging of T cell-dendritic cell interactions in lymph nodes. *Science* **296**, 1873–1876 (2002).
15. Bousso, P. & Robey, E. Dynamics of CD8+ T cell priming by dendritic cells in intact lymph nodes. *Nat. Immunol.* **4**, 579–585 (2003).
16. Hommel, M. & Kyewski, B. Dynamic changes during the immune response in T cell-antigen-presenting cell clusters isolated from lymph nodes. *J. Exp. Med.* **197**, 269–280 (2003).
17. Ingulli, E., Mondino, A., Khoruts, A. & Jenkins, M.K. *In vivo* detection of dendritic cell antigen presentation to CD4+ T cells. *J. Exp. Med.* **185**, 2133–2141 (1997).
18. Doh, J. & Krummel, M.F. Immunological synapses within context: patterns of cell-cell communication and their application in T-T interactions. *Curr. Top. Microbiol. Immunol.* **340**, 25–50 (2010).
19. Skokos, D. *et al.* Peptide-MHC potency governs dynamic interactions between T cells and dendritic cells in lymph nodes. *Nat. Immunol.* **8**, 835–844 (2007).
20. Friedman, R.S., Beemiller, P., Sorensen, C.M., Jacobelli, J. & Krummel, M.F. Real-time analysis of T cell receptors in naive cells *in vitro* and *in vivo* reveals flexibility in synapse and signaling dynamics. *J. Exp. Med.* **207**, 2733–2749 (2010).
21. Marzo, A.L. *et al.* Initial T cell frequency dictates memory CD8+ T cell lineage commitment. *Nat. Immunol.* **6**, 793–799 (2005).
22. Jenkins, M.K. & Moon, J.J. The role of naive T cell precursor frequency and recruitment in dictating immune response magnitude. *J. Immunol.* **188**, 4135–4140 (2012).
23. Gallatin, W.M., Weissman, I.L. & Butcher, E.C. A cell-surface molecule involved in organ-specific homing of lymphocytes. *Nature* **304**, 30–34 (1983).
24. Badovinac, V.P., Messingham, K.A., Jabbari, A., Haring, J.S. & Harty, J.T. Accelerated CD8+ T-cell memory and prime-boost response after dendritic-cell vaccination. *Nat. Med.* **11**, 748–756 (2005).
25. Springer, T.A. & Dustin, M.L. Integrin inside-out signaling and the immunological synapse. *Curr. Opin. Cell Biol.* **24**, 107–115 (2012).
26. Jung, S. *et al.* *In vivo* depletion of CD11c+ dendritic cells abrogates priming of CD8+ T cells by exogenous cell-associated antigens. *Immunity* **17**, 211–220 (2002).
27. Kaech, S.M. & Ahmed, R. Memory CD8+ T cell differentiation: initial antigen encounter triggers a developmental program in naive cells. *Nat. Immunol.* **2**, 415–422 (2001).
28. van Stipdonk, M.J., Lemmens, E.E. & Schoenberger, S.P. Naive CTLs require a single brief period of antigenic stimulation for clonal expansion and differentiation. *Nat. Immunol.* **2**, 423–429 (2001).
29. Wong, P. & Pamer, E.G. Cutting edge: antigen-independent CD8 T cell proliferation. *J. Immunol.* **166**, 5864–5868 (2001).
30. Prlic, M., Hernandez-Hoyos, G. & Bevan, M.J. Duration of the initial TCR stimulus controls the magnitude but not functionality of the CD8+ T cell response. *J. Exp. Med.* **203**, 2135–2143 (2006).
31. Rothlein, R. & Springer, T.A. The requirement for lymphocyte function-associated antigen 1 in homotypic leukocyte adhesion stimulated by phorbol ester. *J. Exp. Med.* **163**, 1132–1149 (1986).
32. Maldonado, R.A. *et al.* Control of T helper cell differentiation through cytokine receptor inclusion in the immunological synapse. *J. Exp. Med.* **206**, 877–892 (2009).
33. Beuneu, H. *et al.* Visualizing the functional diversification of CD8+ T cell responses in lymph nodes. *Immunity* **33**, 412–423 (2010).
34. Sallusto, F., Geginat, J. & Lanzavecchia, A. Central memory and effector memory T cell subsets: function, generation, and maintenance. *Annu. Rev. Immunol.* **22**, 745–763 (2004).
35. Chang, J.T. *et al.* Asymmetric T lymphocyte division in the initiation of adaptive immune responses. *Science* **315**, 1687–1691 (2007).
36. Zhou, L., Chong, M.M. & Littman, D.R. Plasticity of CD4+ T cell lineage differentiation. *Immunity* **30**, 646–655 (2009).
37. Sercan, O., Stoycheva, D., Hammerling, G.J., Arnold, B. & Schuler, T. IFN-γ receptor signaling regulates memory CD8+ T cell differentiation. *J. Immunol.* **184**, 2855–2862 (2010).
38. Perona-Wright, G., Mohrs, K. & Mohrs, M. Sustained signaling by canonical helper T cell cytokines throughout the reactive lymph node. *Nat. Immunol.* **11**, 520–526 (2010).
39. Agarwal, P. *et al.* Gene regulation and chromatin remodeling by IL-12 and type I IFN in programming for CD8 T cell effector function and memory. *J. Immunol.* **183**, 1695–1704 (2009).
40. Haring, J.S., Corbin, G.A. & Harty, J.T. Dynamic regulation of IFN-γ signaling in antigen-specific CD8+ T cells responding to infection. *J. Immunol.* **174**, 6791–6802 (2005).
41. Huang, J.F. *et al.* TCR-Mediated internalization of peptide-MHC complexes acquired by T cells. *Science* **286**, 952–954 (1999).
42. Helft, J. *et al.* Antigen-specific T-T interactions regulate CD4 T-cell expansion. *Blood* **112**, 1249–1258 (2008).
43. Thaventhiran, J.E. *et al.* Activation of the Hippo pathway by CTLA-4 regulates the expression of Blimp-1 in the CD8+ T cell. *Proc. Natl. Acad. Sci. USA* **109**, E2223–E2229 (2012).
44. Seeley, T.S.C. & Sneyd, J. Collective decision making in honey bees: how colonies choose among nectar sources. *Behav. Ecol. Sociobiol.* **28**, 277–290 (1991).
45. Aman, A. & Piotrowski, T. Cell migration during morphogenesis. *Dev. Biol.* **341**, 20–33 (2010).
46. Tsuji, T., Ibaragi, S. & Hu, G.F. Epithelial-mesenchymal transition and cell cooperativity in metastasis. *Cancer Res.* **69**, 7135–7139 (2009).

ONLINE METHODS

Mice. *Icam1*$^{-/-}$ mice (The Jackson Laboratory) were crossed with OT-I (CD45.1^{+}) mice to generate *Icam1*$^{-/-}$ OT-I (CD45.1^{+}) mice, and were crossed with P14 (CD45.1^{+}) mice to generate *Icam1*$^{-/-}$ P14 (CD45.1^{+}) mice. H-2K^{bm1} mice (The Jackson Laboratory) were crossed with OT-I (CD45.1^{+}) mice to generate H-2K^{bm1} OT-I (CD45.1^{+}) mice. Those mice, C57BL/6 mice (The Jackson Laboratory and Simonsen), CD11c-DTR mice, Yet40 (YETI) mice, H-2K^{bm1} mice, CD11c-YFP mice, *Ifngr*$^{-/-}$ mice, P14 CD45.1^{+} mice, CD2-RFP OT-I mice and CD45.1^{+} OT-I mice were housed and bred under specific pathogen–free conditions at the University of California Animal Barrier Facility. All experiments involving mice were approved by the Institutional Animal Care and Use Committee of the University of California.

Cell isolation. OT-I or P14 T cells were isolated from lymph nodes and spleen of 6- to 12-week-old mice. Selection was carried out with a negative CD8 isolation kit (Stemcell Technologies). BMDCs were generated by culture of bone marrow cells for 8–11 d with GM-CSF (granulocyte-macrophage colony-stimulating factor). IL-4 was added for the final 2 d of culture.

Cell transfer, immunization, anti-LFA-1 treatment and recall. OT-I or P14 cells were labeled for 30 min at 37 °C with 2 μM CFSE (carboxyfluorescein diacetate succinimidyl ester; Invitrogen) and then were transferred into recipient mice by retro-orbital injection. Mice were immunized 16 h later. For immunization with DEC-OVA, a complex of anti-DEC-205 (NLDC-145) conjugated to OVA was produce in-house and DEC-OVA conjugates were injected subcutaneously into both flanks of mice in the presence of 10 μg anti-CD40 (1C10; eBiosciences). For immunization with LM-OVA, mice were given intravenous injection of 10×10^3 colony-forming units of *L. monocytogenes* expressing a secreted form of OVA[47]. For immunization with LCMV, mice were given intravenous injection of 1×10^6 plaque-forming units of LCMV (Armstrong strain). For DC-ablation experiments, BMDCs generated from CD11c-DTR mice were pulsed for 30-60 min at 37 °C with 30 ng/ml of the OVA peptide SIINFEKL (AnaSpec). Mice were immunized by subcutaneous injection of 1×10^5 CD11c-DTR BMDCs per flank, in the presence of 200 ng/ml LPS in PBS. At the appropriate time after immunization, diphtheria toxin (Sigma) at a dose of 200 ng per mouse was administered by intraperitoneal injection.

In some experiments, mice received 100–200 μg of isotype-matched control antibody (rat IgG2a; 2A3; BioXCell) or anti-LFA-1 (M17.4; BioXCell) every 12 h for 36 h. For blocking of homing and synchronizing T cell activation, mice were treated with 200 μg anti-CD62L (Mel-14; University of California, San Francisco (UCSF) Hydridoma Core). For recall experiments, mice were rechallenged subcutaneously with 0.2 μg DEC-OVA and 10 μg anti-CD40 at 28–30 d after the primary immunization.

DC vaccination and challenge with LM-OVA. Mice were given transfer of 5×10^3 *Icam1*$^{+/+}$ or *Icam1*$^{-/-}$ OT-I cells and were vaccinated with 2×10^4 SIINFEKL-pulsed BMDCs on both flanks in the presence of 200 ng/ml LPS. Where required, mice received treatment with anti-LFA-1 as described above. In some experiments, OT-I cells were isolated 6 d after vaccination and transferred into naive recipients. At 40–70 d after vaccination, mice were challenged with a lethal dose of LM-OVA (2× to 10× the LD_{50}).

Surface and intracellular flow cytometry staining. Cells were washed in PBS, and nonspecific binding was blocked with flow cytometry buffer (2% FCS, 2 mM EDTA and 0.1% sodium azide in PBS) containing anti-CD16-CD32 (2.4G2; UCSF Hybridoma Core). Surface proteins on cells were stained for 20 min at 4 °C with the following fluorescence-conjugated antibodies in flow cytometry buffer: anti-CD45.1 (A20), anti-CD45.2 (104), anti-CD8 (53.6.72), anti-CD62L (Mel-14), anti-CD44 (IM7), anti-CD69 (H1.2F3) and anti-KLRGI (2F1; all from eBiosciences); and anti-IL-7R (B12-1; Biolegend). Cells were washed and resuspended in flow cytometry buffer containing 1% PFA.

For staining of intracellular cytokines, mice were killed 5 to 6 d after immunization or 4 d after recall. Lymph node cells were restimulated *ex vivo* for 4 h with 100 ng/ml SIINFEKL or 50 ng/ml PMA (phorbol 12-myristate 13-acetate) and 500 ng/ml ionomycin in the presence of 3 μg/ml brefeldinA (Sigma-Aldrich) for the final 2 h. Cells were stained for surface proteins and fixed in flow cytometry buffer plus 2% PFA. Cells were then permeabilized for 5 min with flow cytometry buffer containing 2% saponin and were stained for 15 min at 20 °C with fluorescence-conjugated anti-IFN-γ (XMG1.2; eBiosciences) in flow cytometry buffer and 1% saponin. Cells were kept in flow cytometry buffer and 1% PFA before analysis.

Quantification of endogenous OVA-specific CD8^{+} T cells. Lymph node cells were stained with R-phycoerythrin conjugated to an MHC class I pentamer specific for SIINFEKL (Proimmune) in flow cytometry buffer. Subsequently, cells were stained for CD8 and analyzed by flow cytometry.

***In vitro* T cell priming.** Naive OT-I cells were plated at low density (0.5×10^6 cells per 5 ml) and activated with 2 ng/ml PMA and 20 ng/ml ionomycin. Cells were treated, where appropriate, with 20 μg/ml anti-LFA-1 (M17.4; BioXCell), 20 μg/ml anti-IFN-γ (XMG1.2, BioXCell) and 10 ng/ml or 500 ng/ml IFN-γ (Peprotech). Where appropriate, 2–3 d after priming, cells were transferred into wild-type recipients by retro-orbital injection.

***In vitro* T cell–DC and T cell–T cell clustering assays.** BMDCs were matured with 1 μg/ml LPS 1 d before being pulsed for 30 min with 100 ng/ml SIINFEKL. BMDCs and naive OT-I cells were labeled with 4 μM DDAO (7-hydroxy-9H-(1,3-dichloro-9,9-dimethylacridin-2-one; Invitrogen) and 1 μM CFSE, respectively. Flow cytometry–based coupling was analyzed as described[48].

For T cell–T cell clustering, naive *Icam1*$^{+/+}$ and *Icam1*$^{-/-}$ OT-I cells were labeled with 1 μM CFSE and 2 μM CMTMR (5-(and-6)-(((4-chloromethyl)benzoyl) amino)tetramethylrhodamine; Invitrogen), respectively. Cells were admixed and then were activated with 5 ng/ml PMA and 50 ng/ml ionomycin. After 24 h, cells were fixed in 2% PFA and were analyzed by microscopy or flow cytometry. For flow cytometry, cells were passed through a 40-μm strainer to separate clustered from unclustered cells.

IFN-γ–GFP expression in T cell blasts. Mouse IFN-γ was fused to the GFP via the restriction sites XhoI and AgeI. Then, cDNA encoding that fusion protein was inserted into MSCV plasmid pBabe MCS-IRES-RFP (Addgene) via the restriction sites XhoI and NotI. Naive OT-I cells were activated with 2 μg/ml plate-bound anti-CD3 (2C11; UCSF Hybridoma Core) and 2 μg/ml anti-CD28 (PV1; UCSF Hybridoma Core). The Phoenix packaging cell line was transfected with plasmid encoding IFN-γ–GFP by the calcium-phosphate method. Virus-containing supernatants from these cells were used on two consecutive days (days 2 and 3 after activation) for 'spin-infection' of T cell blasts. Transduced cells were used 4 d after activation.

IFN-γ capture assay and confocal microscopy. OT-I cells were coated with mouse IFN-γ 'catch reagent' from a mouse IFN-γ secretion assay detection kit (Miltenyi Biotec) and were activated with 5 ng/ml PMA and 50 ng/ml ionomycin on fibronectin-coated chambers. After 24 h, cells were fixed for 15 min at 4 °C with 1% PFA and then stained with phycoerythrin- or allophycocyanin-conjugated anti-IFN-γ (detection antibody). Cells were analyzed with an inverted Yokogawa CSU-10 spinning-disk microscope (Zeiss). The imaging and control software used was MetaMorph (MDS Analytical Technologies).

Histology. For cell clustering at low precursor frequency, serial sections (60 μm in thickness) of PFA-fixed and frozen lymph nodes were incubated for 20 min in cold acetone. Total CFSE-labeled or GFP OT-I cells and frequency of clusters were quantified for the whole lymph node. For IFN-γ staining, sections (20 μm in thickness) of PFA-fixed and frozen lymph nodes were stained with anti-IFN-γ (XMG1.2; BioXCell) and Alexa 488–conjugated anti-GFP (A21311; Invitrogen). Sections were then washed and incubated with DyLight 649–conjugated anti-rat (112-496-075; Jackson ImmunoResearch). All sections were analyzed by confocal microscopy.

Two-photon imaging of explanted lymph nodes. For analysis of T cell–clustering kinetics, red fluorescent protein–expressing OT-I cells (3×10^6) were transferred into CD11c-YFP recipient reporter. For analysis of T cell–clustering ability of *Icam1*$^{-/-}$ OT-I cells, *Icam1*$^{+/+}$ and *Icam1*$^{-/-}$ OT-I cells were labeled with 2 μM CFSE and 20 μM CMTMR, respectively, admixed and transferred into wild-type recipient. Switching dyes did not affect results

(data not shown). Mice were immunized subcutaneously in footpads and flanks with 2 μg DEC-OVA and 10 μg anti-CD40 or were left unimmunized as a control. Where appropriate, 150 μg anti-LFA-1 was administered subcutaneously. For analysis of T cell activity after BMDC ablation, $H2b^{bm1}$ OT-I cells were labeled with 2 μM CFSE and transferred into $H2b^{bm1}$ mice. Mice were then immunized with CMTMR-labeled and SIINFEKL-pulsed BMDCs generated from CD11c-DTR mice. Where needed, mice were treated with diphtheria toxin 8 h after immunization. Draining lymph nodes were removed and immobilized on coverslips with the hilum facing away from the objective.

Time-lapse imaging was done with a custom resonant-scanning instrument containing a four-photomultiplier tube (Hamamatsu) operating at video rate, as described[20]. Each *xy* plane spanned 288 μm × 240 μm at a resolution of 0.60 μm per pixel. Images of up to 35 *xy* planes with 3-μm *z*-spacing were acquired every 30 s for 30 min.

Imaris (Bitplane) and Matlab software (Mathworks) were used for quantification of T cell speed and cell clustering. T cell–T cell interaction was defined as the close association of a given OT-I cell with another OT-I cell for at least 3 min. A threshold of 4 μm between cell edges was used, which account for low fluorescence frequently encountered at cell edges, which fit manual quantification (data not shown).

Statistical analysis. Comparisons between groups were analyzed with the *t*-test or one-way or two-way ANOVA, with GraphPrism software. Data were considered significant when *P* values were 0.05 or less.

47. Pope, C. *et al.* Organ-specific regulation of the CD8 T cell response to *Listeria monocytogenes* infection. *J. Immunol.* **166**, 3402–3409 (2001).
48. Friedman, R.S., Jacobelli, J. & Krummel, M.F. Surface-bound chemokines capture and prime T cells for synapse formation. *Nat. Immunol.* **7**, 1101–1108 (2006).

doi:10.1038/ni.2547